Air entrapment in piezo-driven inkjet printheads

Jos de Jong and Gerrit de Bruin
Physics of Fluids Group, Faculty of Science and Technology and Burgers Center of Fluid Dynamics, University of Twente, Enschede, P.O. Box 217, 7500 AE Enschede, The Netherlands

Hans Reinten, Marc van den Berg, and Herman Wijshoff
Océ Technologies B.V., P.O. Box 101, 5900 MA Venlo, The Netherlands

Michel Versluis and Detlef Lohse
Physics of Fluids Group, Faculty of Science and Technology, Burgers Center of Fluid Dynamics, MESA+Institute for Nanotechnology, Institute for Biomedical Technology (BMTI) and Institute of Mechanics, Processes and Control-Twente (IMPACT), University of Twente, P.O. Box 217, 7500 AE Enschede, The Netherlands

(Received 31 May 2005; revised 22 May 2006; accepted 25 May 2006)

The stability of inkjet printers is a major requirement for high-quality-printing. However, in piezo-driven inkjet printheads, air entrapment can lead to malfunctioning of the jet formation. The piezoactuator is employed to actively monitor the channel acoustics and to identify distortions at an early stage. Modifications of the response of the piezoactuator indicate entrapped air bubbles and these allow us to investigate them. When we employ the signal as a trigger for high-speed imaging, we can visualize the consequences of the entrained bubbles on the droplet formation. Two mechanisms are found to cause air entrapment: First, a distorted droplet formation caused by small particles, and, second, an accumulation of ink on the nozzle plate, which favors void formation once the meniscus is pulled back. © *2006 Acoustical Society of America.* [DOI: 10.1121/1.2216560]

PACS number(s): 43.25.Yw, 43.38.Fx, 43.35.-c [AJS] Pages: 1257–1265

I. INTRODUCTION

Today's drop-on-demand inkjet printers[1] have as crucial requirements that they are fast, can produce small droplets, and are reliable and robust against distortions. For one full-color A0 print, up to one billion droplets are required. The failure of only a few drops could jeopardize the whole result.

Though in principle inkjet printing with piezoelectric actuation[1] can fulfill all of the above requirements, sometimes, even when the droplet forming process may be very stable for literally millions of droplets, from one to the next actuation cycle there may be an occurrence giving rise to a malfunction of the droplet formation. In the modern versions droplets are jetted every 50 μs. Therefore, for the early detection of anomalies, monitoring of the printing process *while printing* becomes crucial.

In piezoelectric printheads the piezoceramic material is deformed, resulting in pressure buildup at the nozzle region, which is released through drop formation at the nozzle. Fluid acoustics are involved to guide the waveform energy toward the nozzle, and to create pressure and velocity profiles needed for the droplet jetting process.[2] For the discussion of different types of piezoelectric drop-on-demand systems and their principles we refer to Refs. 3–10.

In this paper we will focus on the malfunction of piezoelectric printheads and introduce a method to acoustically detect them at an early stage. It is known that the formation of *air bubbles* during operation can be the origin of the failure of the piezoelectric inkjet system.[11,12] These bubbles alter the acoustic field required for the droplet formation and in many cases cause the droplet formation to stop completely. The bubble only dissolves when the acoustic field is turned off, bringing the total print process to an end. Obviously, first, an early detection of the bubble is desirable, so that, second, some measures can be taken to get rid of the bubble.

In this paper we address the first point and present a measurement technique to acoustically monitor the ink channel and to detect air bubbles therein while printing. This active monitoring is performed by using the piezoelement as a sensor, measuring the pressure in the channel between the droplet-firing pulses by the same piezo. The electrical signal measured from the piezo will be referred to as the acoustical signal in this article. The acoustical signal actively monitors the droplet formation and reacts within microseconds to any change in the acoustical signal. We can therefore use this signal to trigger a high speed camera with which we image the droplet formation process. The high-speed images are correlated with the acoustical signal.

How do the bubbles enter into the ink channel? The origin of the air bubbles can be either nucleation inside the ink channel or air entrapment at the nozzle. As the absence of large pressure amplitudes in the ink channel rules out the first mechanism, we focus on air bubbles entrapped at the nozzle. Once entrapped, the bubble will grow by rectified diffusion[13–15] under the influence of the acoustic actuations, resulting in malfunctioning of the printhead. We will also address the consequences for the functioning of the printhead, in particular, the effect of the entrapped air bubble on the droplet speed. From the high speed imaging of the droplet formation and the air entrapment process, we identify two air entrapment mechanisms:

- a distorted droplet formation caused by small (dust) particles

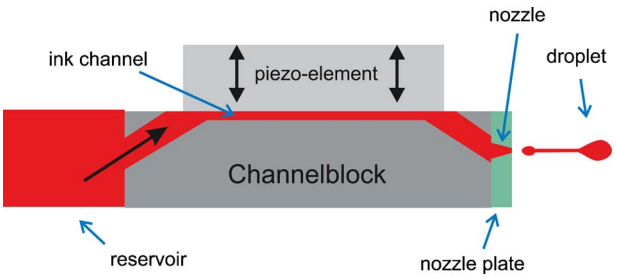

FIG. 1. (Color online) Sketch of the geometry of the printhead. The reservoir is pressure controlled, pushing ink into the rectangular ink channel of the typical length of 10 mm, width of 200 μm, and height of 150 μm. The piezoelement of length 8 mm is covered with a foil of 20 μm thickness, which is in direct contact with the ink. The nozzle plate is nickel-made with round openings of diameter 30 μm, the nozzles themselves. The jetted droplets have a diameter of typically 35 μm.

- creating an ink layer on the nozzle plate, which favors void formation once the meniscus is pulled back and the ink closes the void

The paper is organized as follows: In Sec. II we explain the printhead setup and its operation. In Sec. III we present results on the acoustical bubble detection technique. Section IV is devoted to the high-speed imaging of droplet formation, which is triggered once the acoustical signal gets distorted. In Sec. V we identify the two above mentioned ways how bubbles are entrained in the nozzle. The last section is left to discussions, conclusions, and an outlook.

II. PRINTHEAD SETUP AND OPERATION

The printheads under consideration in this paper are side-shooter printheads developed by Océ and used for professional printing in an industrial environment. The schematic setup of the printhead is depicted in Fig. 1. The channel block is a graphite block with ink channels inside. The ink reservoir is connected to the channel and can be set at a specific ambient pressure. For example, to prevent ink leakage from the nozzles when not jetting, the ambient pressure in the reservoir is lowered, typically by 8 mbar. In the rectangular ink channel, one of the four walls is formed by the piezo. When a voltage pulse is applied to the piezo, the piezo first contracts, increasing the volume of the ink channel. This results in a lower pressure in the channel. In the second part of the pulse, the piezo is expanded again, reducing the volume of the ink channel and thus pushing ink therein, resulting in a buildup of (positive) pressure ("push mode"). The pressure waves generated by the piezo travel toward the ink reservoir, where they are reflected out of phase, and toward the nozzle, where they are reflected in phase. The ink is pressed out through a 30 μm diameter electroformed nickel nozzle.

The printhead driving protocol is sketched in Fig. 2. The applied pulse is a trapezium pulse with a total length of about 15 μs, and the repetition rate of the pulse is 20 kHz (corresponding to 50 μs pulse to pulse distance), which is the firing frequency of the droplets. When the piezo is no longer actuated, it is employed to monitor the pressure waves inside

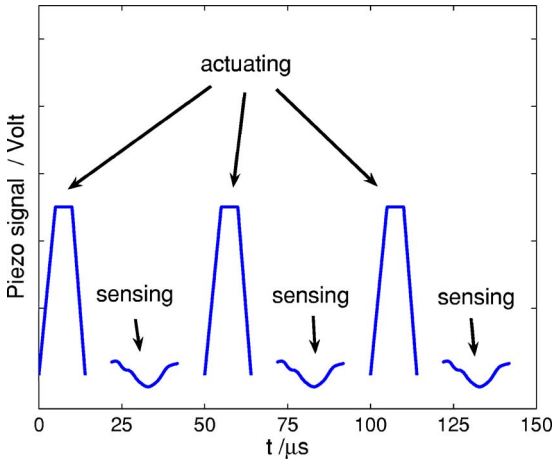

FIG. 2. (Color online) Schematic drawing of the piezo signals. Ink is pressed out of the nozzle through short pressure pulses of 15 μs width, being typically 50 μs apart (i.e., 20 kHz drop printing frequency). In between the pressure pulses the piezoelement is used as a pressure sensor.

the ink channel. The switching from actuating to sensing and vice versa takes about 5 μs and the temporal resolution of the signal is 0.1 μs.

To convey a qualitative idea on the normal operation of the printhead and the droplet formation process, we have modeled the three dimensional ink channel and the nozzle with the CFD program Flow-3D.[16] This CFD code uses a Volume of Fluid technique.[17] The piezo is simulated by a moving obstacle at one side of the ink channel. This compressible model incorporates viscosity and surface tension. It is also considered that the graphite walls of the channel are not stiff, leading to a reduction of the effective sound velocity. Details on the employed numerical model can be found in the articles of Hirt[17] and of Wijshoff.[19] In Fig. 3 the experimental (upper) and numerical (lower) droplet formation processes are compared. They show reasonable qualitative agreement. A small deviation is seen at the breakup of the droplet. This deviation is presumably caused by noise in the actual droplet formation[18] and by the finite mesh size of the model. However, we stress again that no quantitative comparison is aimed at, at this point.

III. ACOUSTICAL DETECTION OF AIR BUBBLES

As pointed out in the previous section and sketched in Fig. 2, the roughly 30 μs long period between pressure pulses is employed to monitor the channel acoustics. This is possible because the acoustic pressure waves present in the ink channel deform the piezo. The force exerted on the piezoelement is converted to an electrical signal that we call the acoustical signal,[24]

$$a(t) = \int_{\text{piezo}} \frac{dF}{dt} dA .$$

Here, $F(t)$ is the force exerted on the piezo, perpendicular to the ink channel. Its temporal change is integrated over the surface A of the piezo, which is in direct contact with the ink. The piezo is nearly as long as the ink channel (8 vs 10 mm total length). Therefore the signal integrates the forces

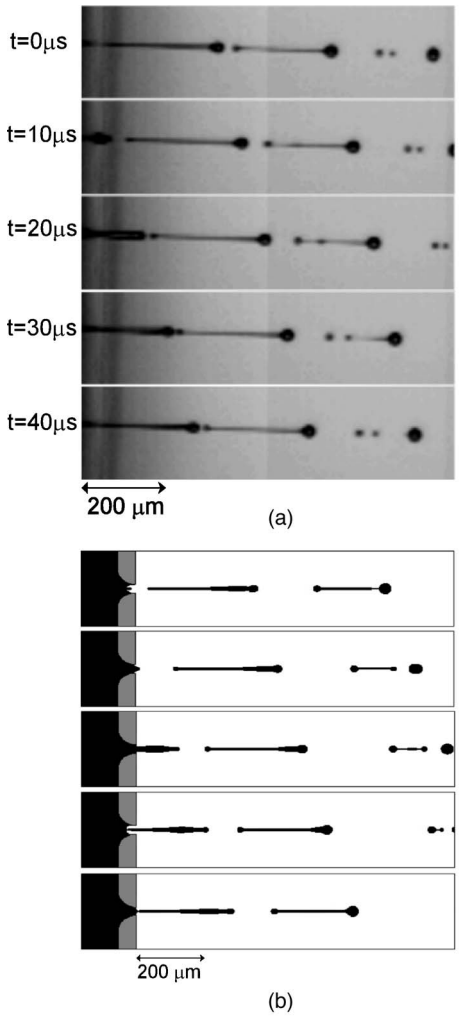

FIG. 3. A comparison of the droplet formation at 20 kHz. (a) Droplet formation, recorded by high speed imaging, (b) Droplet formation, simulated with Flow-3D. The same piezo-deformation as in experiment has been chosen, leading to the pressure profile in the ink channel. In both the experimental and the numerical case the droplet velocity is about 7 m/s.

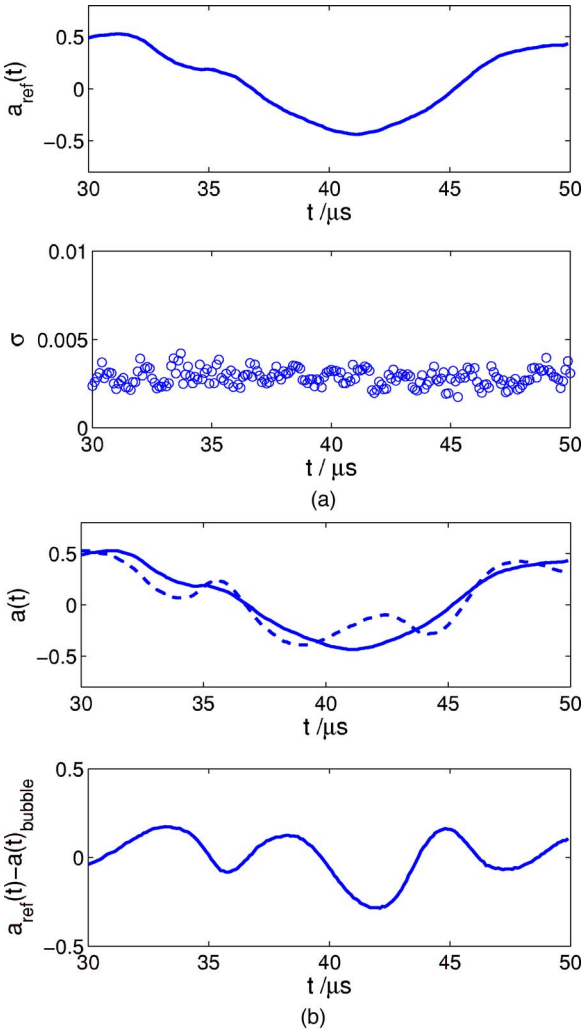

FIG. 4. (a) (Color online) The acoustical signal, $a_{ref}(t)$, averaged over 25 standard droplets (upper), and the corresponding standard deviation that is more than 100 times smaller (lower), showing the reproducibility of the signal. Note the 50 times enlarged scale on the y axis. (b) Upper: Acoustical signals with (dashed) and without (solid) an air bubble present in the ink channel. The lower panel shows the difference of these two signals.

over the whole length and cannot be directly translated back to the acoustic pressure. However, provided that the droplet is fired without distortion, the signal is perfectly reproducible. This is demonstrated in Fig. 4(a). In the top figure the acoustical signals of 25 successively jetted droplets are displayed. The standard deviation for the 25 signals is calculated in the bottom plot of Fig. 4(a). The standard deviation stays well under 0.005 (less than one percent of the maximal acoustical signal), showing the close to perfect reproducibility of the acoustical signals. Therefore this method is potentially very well suited to monitor flow deviations in the channel and at the nozzle.

As an entrained air bubble modifies the acoustical signal in a characteristic way, above acoustical monitoring method should also reveal when an air bubble is present inside the ink channel. In Fig. 4(b) we present such a case: The top figure displays both the standard acoustical signal (solid line) and the acoustical signal with an entrapped air bubble (dashed line). The modification of the signal caused by the entrapped air bubble is shown in the bottom figure. It can clearly be seen that the air bubble adds an additional frequency component to the acoustical signal. Further evidence that the signal modification is due to a bubble is obtained from the following experiment: The acoustic field is turned off for a specific time interval when the modification is present. If the time interval is long enough for the bubble to entirely dissolve, the signal modification disappears. When the bubble is not completely dissolved once the actuation is resumed; the bubble will again grow by rectified diffusion and cause nozzle failure.

Of course, the acoustic sensoring method allows only for an indirect detection of the bubble, not a direct visualization. Such a visualization is not possible in standard ink channels, as they are optically not accessible. However, recently we have succeeded in direct high-speed visualization of entrained air bubbles in channels equipped with nozzle plates partly made out of glass. A correlation between these images and the acoustical signal fully confirms our interpretation that the origin of the modified acoustical signal are entrained air bubbles.[23]

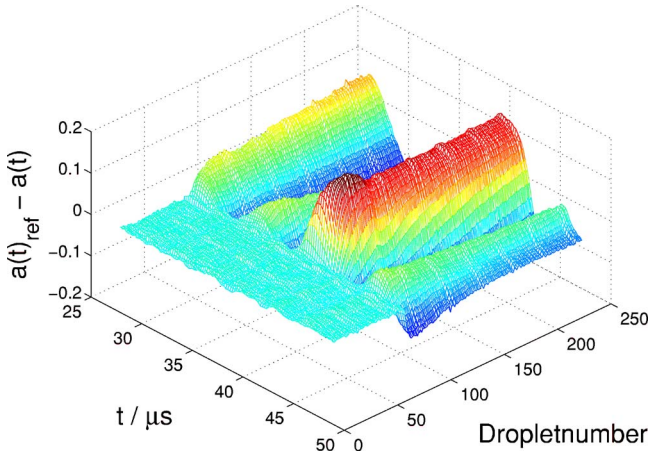

FIG. 5. (Color online) Development of the acoustical signal $a(t)$, as compared to the reference signal $a_{\mathrm{ref}}(t)$ without a bubble, after air bubble entrapment.

The development of the acoustical signal after entrapment of an air bubble is shown in Fig. 5. The difference compared to the reference acoustical signal (i.e., the signal without air bubbles) is plotted. This difference occurs rather suddenly, within only a few cycles. This development of the acoustical signal corresponds to the moving and growing of the air bubble. The bubble growth is presumably due to rectified diffusion, which causes a net flow of dissolved air into the bubble during one acoustic cycle. The larger the bubble, the more it influences the acoustic waves traveling in the ink channel. Before a stationary state of the acoustical signals and therefore presumably also the bubble is reached, it can take several thousands of cycles.

To analyze the acoustical signal, the variance

$$\sigma^2 = \frac{1}{T}\int_0^T [a(t) - \bar{a}]^2\, dt,$$

over one period $T=50$ μs of the acoustical signal is calculated and plotted versus the droplet number; see Fig. 6. Remarkably, a large disturbance during two acoustic cycles is occurring just before air entrapment. This disturbance in the variance corresponds to a variation of only 2% in the amplitude of the acoustical signal. It is perfectly reproducibly, i.e., always occurs before air entrapment. On the other hand, not all these disturbances actually lead to air entrapment (as will be seen from Fig. 9, later). As shown by a trigger based on the variance, the disturbances occur randomly during actuations, and, in fact, only rarely result in air entrapment. What is the origin of this disturbance in the acoustical signal, which seems to be a necessary (but not sufficient) condition for air entrapment?

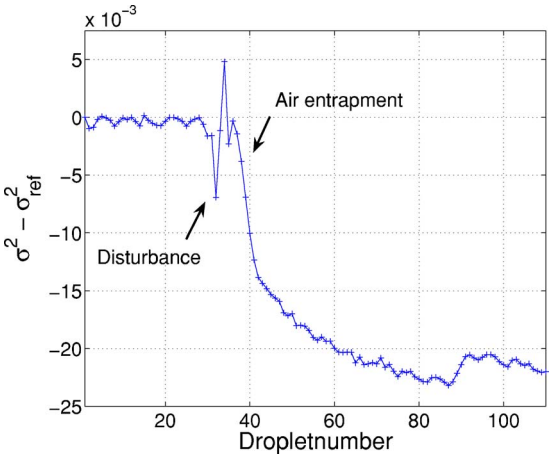

FIG. 6. (Color online) Variance of acoustical signals, when air is entrapped. First the acoustical signals show undisturbed droplets, then a disturbance occurs, and after the disturbance air is entrapped. The variance of the reference signal is subtracted.

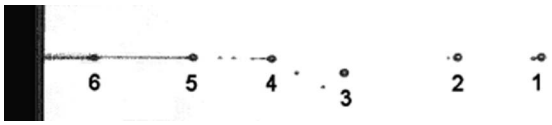

FIG. 7. Distorted droplet formation. Droplets 1 and 2 are standard droplets, droplet 3 corresponds to a disturbance of the acoustical signal (such as, e.g., seen in Fig. 6 for droplets number 34–36 of that figure). Here droplets 4–6 are standard again, but an air bubble is now present in the nozzle. After hundreds of cycles, this can lead to the breakdown of the jetting process.

IV. VISUALIZATION OF DROPLET FORMATION

To answer this question, high speed imaging is employed to visualize the droplets, once the deviation of the variance is detected in the acoustical signal. A Phantom V7 high speed camera from Vision Research is used to monitor the firing of the droplets. The camera is capable of making recordings up to 160 kfps and has pre- and post-triggering. The camera is triggered by the acoustical signal: After a disturbance in the variance has been detected, it records hundreds of droplets before and after the acoustical signal deviation. What can be seen is that the droplet formation is slightly altered before air is entrapped. The droplets differ in speed and sometimes the droplet has a deviant angle. A typical example is shown in Fig. 7.

The first two droplets (1) and (2) are standard droplets. Then a disturbance occurs in droplet (3), which corresponds to the disturbance in the variance shown in Fig. 6. The droplets fired after the disturbance seem to be standard again, but now an air bubble is present inside the nozzle, which can be concluded from the acoustical signal. (The actual air entrapment mechanism will be explained in the next section.) Just after the entrapment the air bubble is presumably very small. Therefore it has a relatively small influence on the droplet formation. After the air bubble is entrapped, it will grow by rectified diffusion and the speed of the droplets is gradually reducing. This is a relatively long-term effect due to the slow time scale of (rectified) diffusion. This can be seen in Fig. 8. The droplet speed reduces by 15% from 6.5 to 5.5 m/s within 20 ms, which corresponds to 400 actuations.

V. ORIGIN OF THE ENTRAINED BUBBLE

A. Air entrapment with regular jetting

As shown in the previous section, it is clear that distorted droplet formation can result in air entrapment. To find out what the actual disturbance is, recordings are made with the Phantom V7 high speed camera. Again, the acoustical signal is used to monitor the droplet formation and to trigger

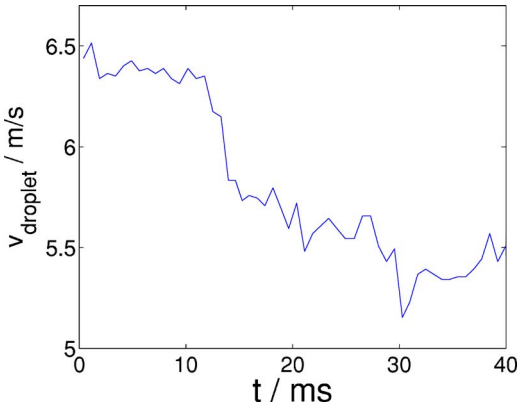

FIG. 8. (Color online) Droplet velocity as a function of time. When an air bubble is entrapped at $t=0$, the droplet speed decreases from 6.5 to 5.5 m/s within 20 ms, corresponding to 400 actuation cycles.

the camera. The shutter was set to 2 μs to prevent motion blur. A typical example recorded with 100 kfps is shown in Fig. 9(a). The corresponding variance of the acoustical signal is plotted in Fig. 9(b). Droplet 26 was created normally, but droplet 27 has a small twist in the tail of the drop. The reason becomes clear when looking at droplet 28, which shows a large disturbance being jetted out. This disturbance caused the droplet formation of droplet 27 to be modified before it was jetted out in the next actuation. After this the droplet formation returns to normal.

Figure 9 typifies a disturbance that potentially leads to air entrapment. To find the origin of the disturbance, some deviating droplets were caught and analyzed with a microscope. The capturing of the droplets was done by creating a piezoelectric device that can move several microns within several microseconds. A microscope glass cover was attached to the tip of the piezoelectric device. This device was placed beneath the nozzle plate, a few microns away from the stream of droplets. The acoustical signal was used as a trigger for the piezoelectric device. When triggered, the piezo moves into the droplet stream and captures a single droplet on the glass cover. This glass cover was then removed from the piezoelectric device and placed under a microscope. The captured transparent ink droplets contain relatively large particles (± 20 μm) that are not present in undisturbed droplets. It is therefore believed that these particles disturb the normal jetting process by creating an asymmetric meniscus, which then could lead to the entrapment of air. The chance of air entrapment depends on the actual position of the particle and the precise time within an acoustical cycle. We conclude that small particles in the ink can result in an altered droplet formation, which then can result into air entrapment.

B. Air entrapment with an ink layer

An ink layer on the nozzle plate can also induce air entrapment while jetting droplets. Therefore experiments are set up to clarify the exact role of an ink layer on air entrapment. During the experiments the time between consecutive actuations, and thus the created droplets, is kept constant at 100 μs. The ink layer is created by applying a higher ambient pressure to the ink reservoir inside the printhead for about one second (typically, $\Delta p = 100$ mbar enhancement, as compared to the standard slight reduction of 8 mbar, which under operational conditions is employed to avoid ink leakage from the nozzles; see Sec. II). This higher ambient pressure is negligible compared to the pressure created by the piezos of the actuated channels. It results in ink flowing out of the nonactuating neighboring nozzles onto the nozzle

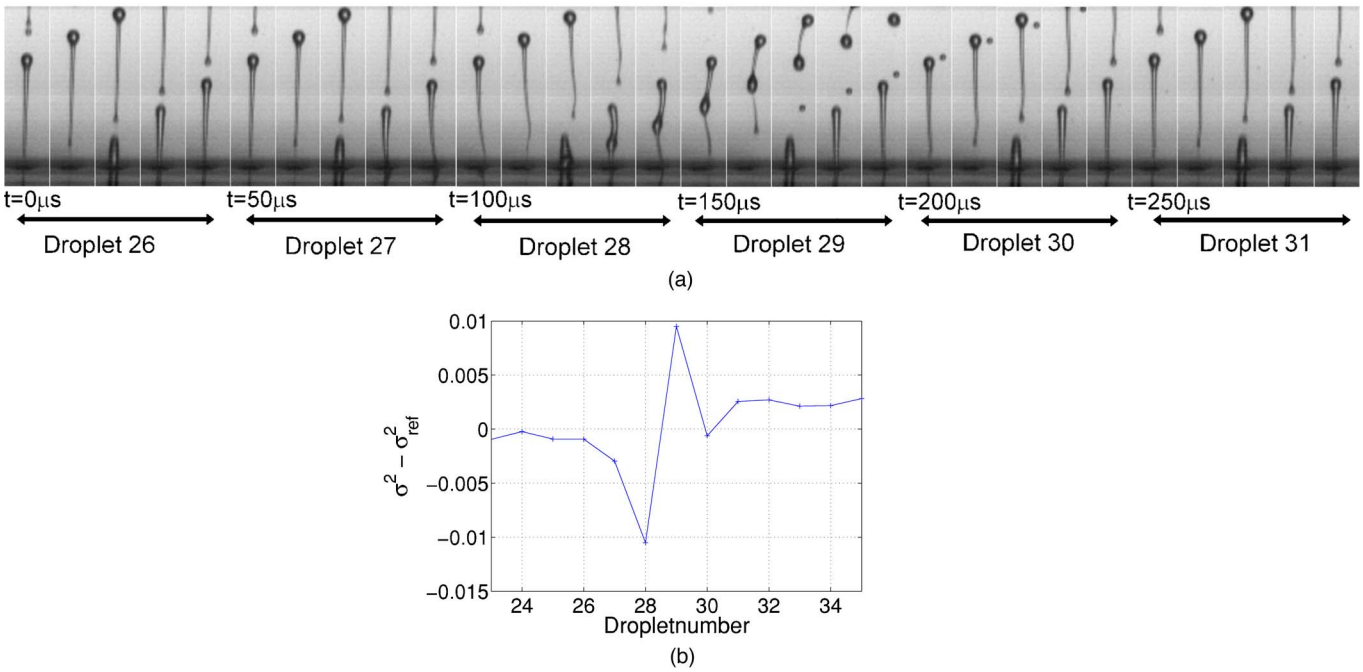

FIG. 9. (Color online) (a) Droplet formation recorded at 100 kfps showing the disturbance that can result in air entrapment. Droplet 26 shows regular droplet formation. Droplet 27 displays a slight deviation in the tail. Droplet 28 shows a large disturbance being jetted out. Droplets 29 and 30 display regular droplet formation again. (b) The variance of the acoustical signals is plotted for the corresponding droplets. The variance signals a large deviation at droplets 27 and 28, corresponding to the disturbance in the droplet formation process.

plate. The ink flows over the nozzle plate and reaches the jetting nozzle. Its effect on the droplet formation is documented in Fig. 10: The ink layer causes a reduction of the droplet velocity. The jet speed reduces with increasing ink layer thickness. At a critical ink layer thickness d_2 the nozzle ceases to fire droplets. When the pressure applied to the ink reservoir is back to its slightly reduced value, the surrounding nozzles suck the ink back into the ink channels. When the ink layer becomes thinner, at the critical thickness d_2 droplets can be jetted again. Finally, the ink layer on the nozzle plate is fully removed. However, it turns out that now air is entrapped in the actuating ink channel. This can be seen in the acoustical signal, such as shown in Fig. 4(b), but also by the lower droplet velocity, which is caused by the acoustical damping through the air bubble. Therefore it is concluded that an ink layer thickness window, $d_1 < d < d_2$, exists, in which air bubbles are entrapped. For smaller thicknesses, $d < d_1$, in general, there is no air entrapment, and for larger thicknesses, $d > d_2$, the meniscus motion is neither sufficient to jet droplets nor to entrap air.

Two typical examples of this process recorded at 10 kfps are shown in Fig. 10 (side view) and in Fig. 11 (top view). Notice the air bubbles on the nozzle plate in the last image of Fig. 11. When the air bubbles are on the nozzle plate, they slowly dissolve in the ink layer, as the pressure fluctuations are not sufficient to support growth by rectified diffusion. As several air bubbles turn up on the nozzle plate, apparently not only one air bubble has been entrapped in the ink channel. This is probably caused by the difference in time scale between the changing of the thickness of the ink layer and the actuation. As the change in the ink layer thickness occurs slowly compared to the actuation frequency, an ink layer with thickness $d_1 < d < d_2$ is present during multiple actuations. If an actuation occurs while the ink layer is within this thickness range, an air bubble is created. So multiple actuations lead to multiple air bubbles. The size of the air bubbles could possibly even reveal information on whether it has moved into the ink channel or has remained on the nozzle plate.

Though these measurements show the existence of an ink layer thickness window for air entrapment, they do not allow us to determine the exact values of the critical thicknesses d_1 and d_2, since the ink layer thickness varies over the nozzle plate. The determination of the critical thicknesses d_1 and d_2 is the subject of the next subsection.

C. Determination of the critical ink layer thickness

In order to find out and to determine the ink layer thicknesses where air entrapment occurs, an additional electroformed nickel nozzle plate is placed on top of the original nozzle plate, as shown in Fig. 12. Different thicknesses of the additional nozzle plate are used to vary the ink layer thickness.

One problem, however, arises: The volume of the additional nozzle is small compared to the volume of a complete ink layer. While jetting, the droplet formation could also change the amount of ink in the additional nickel nozzle of Fig. 12. To overcome this problem, a burst of actuations is

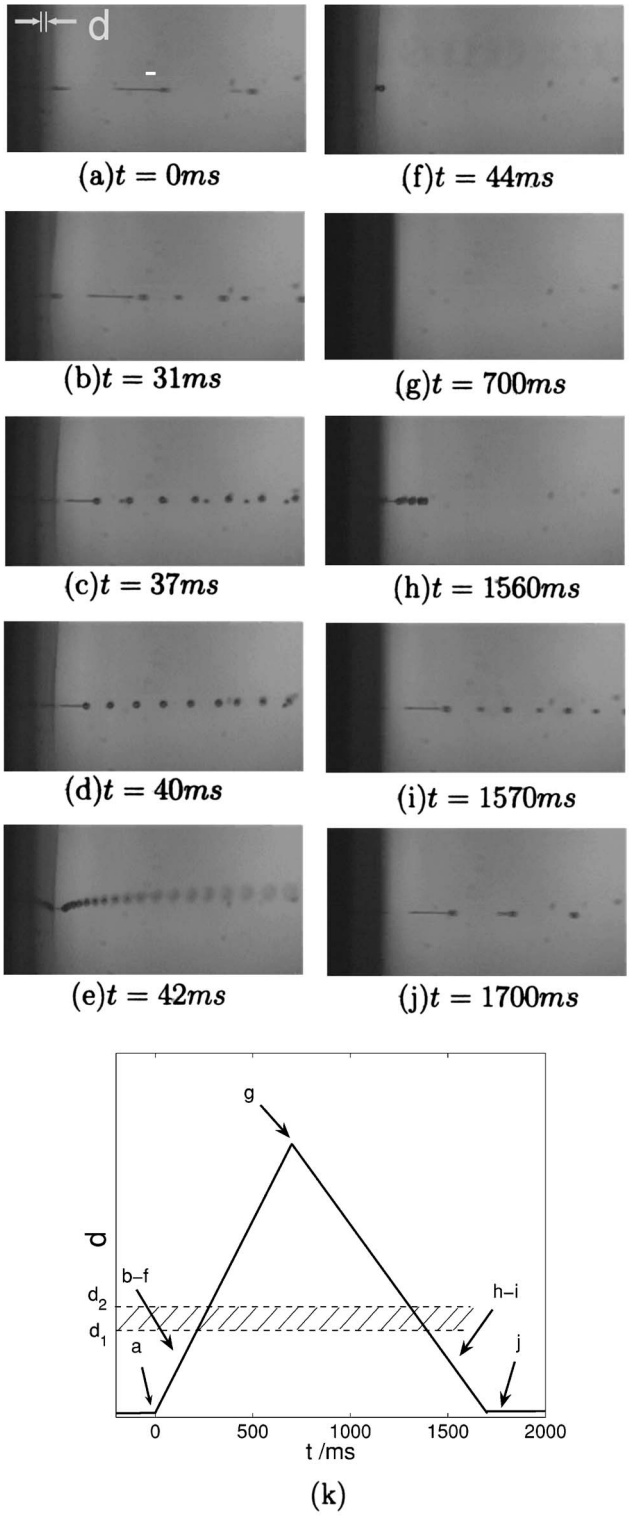

FIG. 10. High speed recordings at 10 kfps of droplets when a temporary ink layer is created on the nozzle plate by applying a higher ambient pressure to the ink reservoir for 700 ms. (a) Regular jetting behavior with no ink layer present. (b)–(e) The higher ambient pressure is applied, resulting in a growing ink layer. The velocity of the droplets is reduced through the ink layer. (f) No droplets are jetted anymore because all acoustic energy is dissipated in the ink layer. (g) The ink layer is very thick and no droplets are created at all. (h)–(j) The enhancement of the ambient pressure has ended, resulting in a reducing ink layer thickness. When the layer is thin enough, the jetting starts again, but now with an air bubble in the ink channel. (k) A schematic diagram of the increasing and decreasing ink layer.

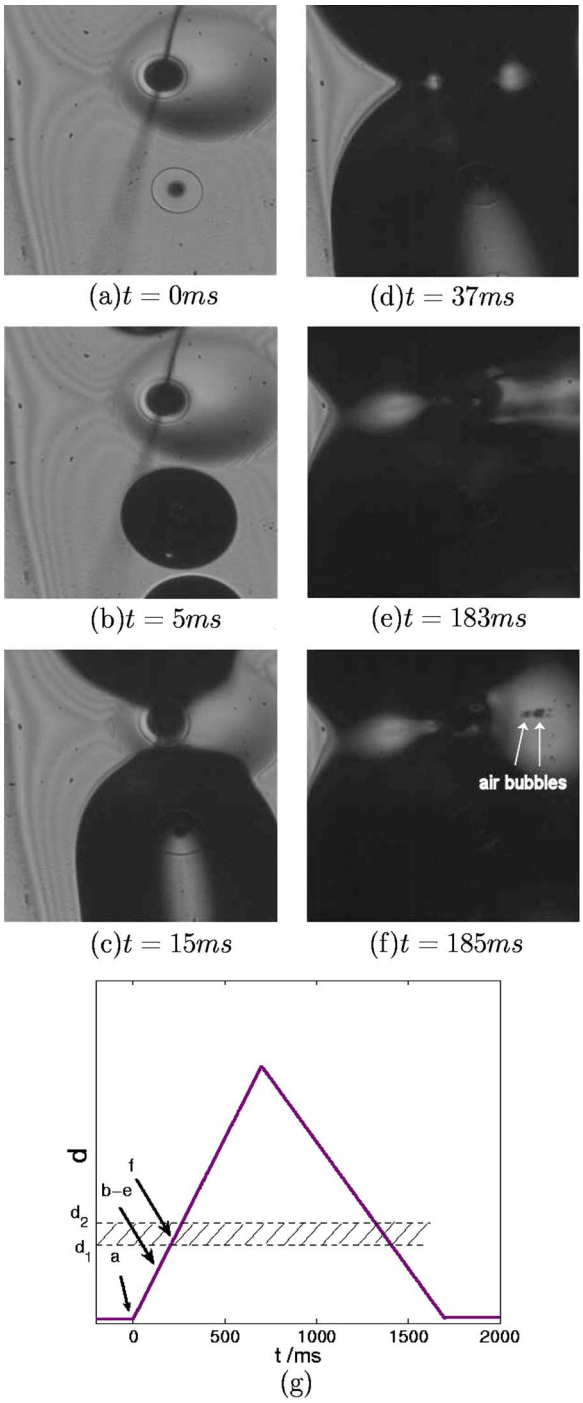

FIG. 11. High speed recordings of droplets at 10 kfps when a temporary ink layer is created on the nozzle plate by applying a higher ambient pressure to the ink reservoir for 700 ms. (a) Normal jetting with no ink layer present. (b)–(d) The higher ambient pressure is applied and the ink layer on the nozzle plate is growing. (e) The droplets now have a reduced speed and a deviant angle of jetting. (f) When the ink layer reaches the critical thickness d_1, air bubbles are created and are present on the nozzle plate. For $d > d_2$ jetting completely breaks down. (g) A schematic diagram of the increasing and decreasing ink layer.

applied. The burst consists of three actuations, after which a waiting period of 3 ms is set. The three actuations are chosen because not only air has to be entrapped, but the air bubble also needs to be detected through the acoustical signal. By controlling the ambient pressure of the ink reservoir, it is ensured that the additional nozzles (Fig. 12) are completely

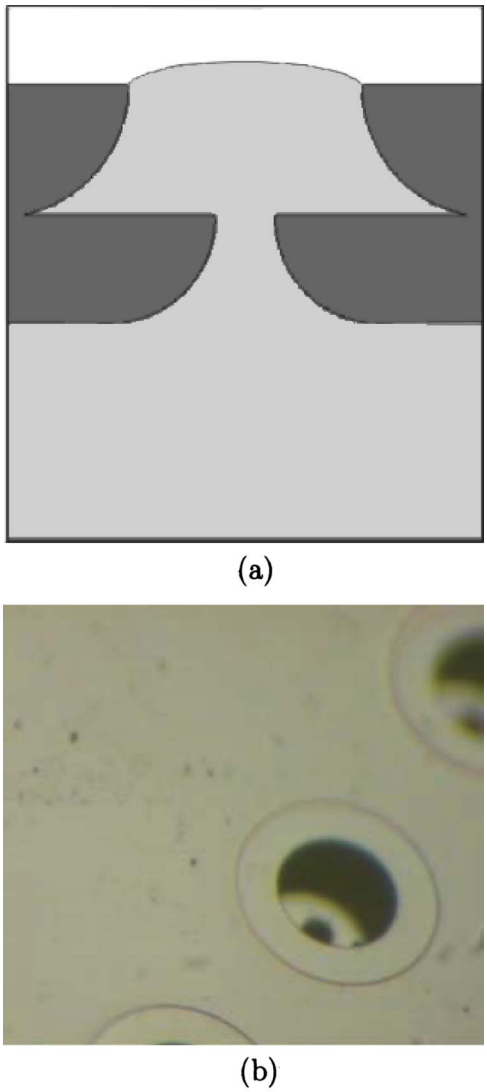

FIG. 12. (Color online) (a) Schematic side view of the additional nozzle plate on top of the original one. (b) Top view photograph of the setup.

filled by the setting of the ambient pressure of the ink reservoir. Measurements show that when the ink layer is relatively thin (<30 μm), or relatively thick (>40 μm), no air entrapment occurs. The region in between is the ink layer thickness window where air entrapment occurs.

D. Numerical simulations on ink layer triggered air entrainment

To qualitatively check whether air entrapment induced by ink layers on the nozzle is also reflected in numerical simulations, a Flow-3D simulation is set up, similar to the one described in Sec. II. For this simulation an ink layer is positioned on the nozzle plate with a thickness of 30 μm. It is assumed that the influence of the ink layer on the acoustical waves inside the printhead is negligible. Two actuations are modeled.

The result is presented in Fig. 13. It can be seen that indeed no air is entrapped during the first acoustic cycle, which lasts for 50 μs. During the second acoustic cycle, air is, however, entrapped. The reason for the delay is that the simulation is started with no fluid movement at all. The ac-

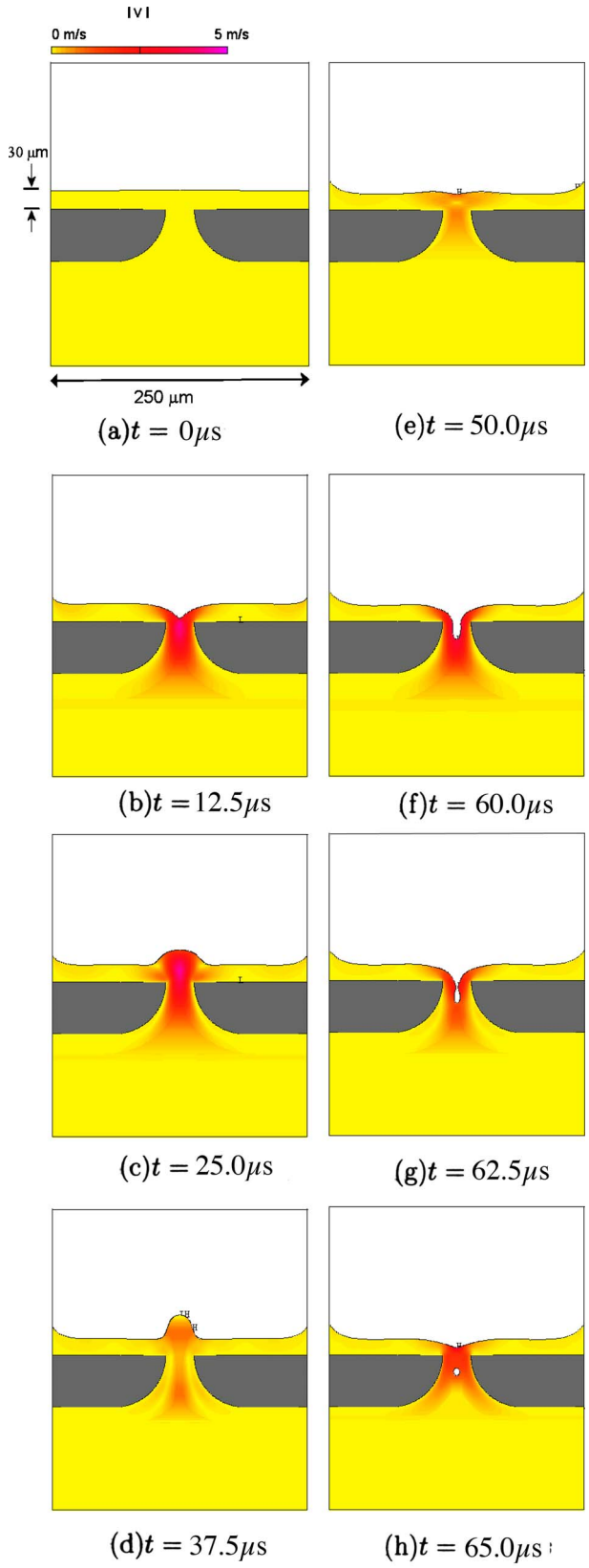

FIG. 13. (Color online) Air entrapment with an ink layer simulated with Flow-3D. (a) A 30 μm ink layer is placed on the nozzle plate. The actuation starts at $t=0$ μs. (b) The meniscus is pulling back due to the first negative pressure wave. (c)–(d) The positive pressure waves pushes the ink out of the nozzle. (e) Start of the second actuation. (f) The negative pressure wave pulls back the meniscus. (g) Due to the larger surrounding pressure, the void is closed. (h) An air bubble is entrapped.

tual air entrapment occurs when the meniscus is pulling back and ink is flowing into the nozzle. If no ink layer was present, the meniscus would retract into the nozzle. However, in the case of an ink layer, also the ink on top of the nozzle plate is pulled into the nozzle. The void is then closed at the top because of the ink flowing in from the sides due to the overpressure.

VI. SUMMARY, DISCUSSION, CONCLUSIONS, AND OUTLOOK

By using the piezoactuator as a sensor, the channel acoustics and the droplet formation can be accurately monitored. In particular, disturbances that can result in air entrapment and the entrapped bubbles themselves are detected by the acoustical signal. Since hitherto the only solution for recovering the regular droplet formation process is the dissolution of the bubble, it is crucial to detect the bubble as soon as possible after entrapment. In that case the bubble has not yet grown by rectified diffusion, and its dissolution time is therefore shorter. By employing the acoustical signal as a trigger, two air entrapment mechanisms are found:

- Air entrapment triggered by particles in the ink, disrupting the droplet formation
- Air entrapment caused by an ink layer on top of the nozzle plate

The first mechanism shows that particles in the ink, for example dust particles, can influence the droplet formation in such a way that air is entrapped. The size of the particles was found to be around 20 μm. Other sized particles will not result in air entrapment since small particles ($\ll$20 μm) will have no influence at all, and large particles ($\gg$20 μm) will block the nozzle and thus the droplet formation. The 20 μm particles probably cause a local surface tension distortion and thus an asymmetry of the droplet formation. This asymmetry of the completely retracted meniscus in combination with the next symmetric pressure wave then could cause air entrapment. The timing, size, and position of the particle is expected to play a crucial role in the air entrapment mechanism.

In the second mechanism an ink layer on top of the nozzle plate of approximately 30–40 μm results in air entrapment. When the meniscus is pulled back due to the negative pressure inside the nozzle, ink from the nozzle plate flows into the nozzle and air is entrapped. This process is modeled with Flow-3D. Measurements show that not all the air bubbles enter the ink channel, but some also move onto the nozzle plate. The exact criterium for entering the nozzle is not clear. Probably parameters like the size, position, and timing play an important role.

Note that small air bubbles cause no problems in jetting. Only once they grow, problems arise. The air bubble starts to oscillate due to the acoustical waves. Because of the oscillations, the bubble will experience a net force directed into the ink channel, the primary Bjerknes force. The oscillations also cause the bubble to grow by rectified diffusion. The further the bubbles moves into the ink channel, the larger the pressure amplitude and therefore also the oscillations and the

growth of the bubble. Note that the properties of bubbles in a constrained geometry such as the ink channel can differ considerably from those of free bubbles.[20–22]

In this paper a method to detect air bubbles in piezo-driven printheads is presented and mechanisms of how bubbles are entrained are identified. From a practical point of view the ultimate goal, of course, must be to prevent air entrapment (or to immediately get rid of the entrained bubbles), in order to improve the jetting stability. The two identified air-entrainment mechanisms suggest two requirements:

- Particles with a size of 20 μm or larger should be prevented to reach the nozzle. Inside the printhead, this can be achieved through filters. But dust particles from outside also form a threat. Printing in a clean environment should prevent particles reaching the nozzle. Fortunately, for printers in an industrial environment it is often possible to control the cleanness of the ambient air (clean-room facilities).
- The ink layer on the nozzle plate should stay below a thickness of 30 μm. This may be accomplished by a special design of the nozzle plates.

More research is needed to clarify the process from air entrapment of a small bubble to a full grown bubble, which eventually prevents the normal jetting of droplets. We have meanwhile optically monitored the trajectory, growth, and size of the bubble with high-speed imaging.[23] The next step is to understand its effect on the pressure field, in order to quantitatively describe the reduction of the droplet jetting velocity and to find out the exact conditions when the jetting will totally break down. Research in this direction is on its way.

ACKNOWLEDGMENTS

We thank the staff of Océ Technologies B.V. for support and Andrea Prosperetti for discussions. This study has been financed by the Fundamenteel Onderzoek der Materie (FOM) of The Netherlands under Grant. No. 02MFS39 and by Océ Technologies B.V.

[1]H. P. Le, "Progress and trends in ink-jet printing technology," J. Imaging Sci. Technol. **42**, 49 (1998).
[2]D. B. Bogy and F. E. Talke, "Experimental and theoretical study of wave propagation phenomena in drop-on-demand ink jet devices," IBM J. Res. Dev. **28**, 314–320 (1984).
[3]J. M. Meacham, M. J. Varady, F. L. Degertekin, and A. G. Fedorov, "Droplet formation and ejection from a micromachined ultrasonic droplet generator: Visualization and scaling," Phys. Fluids **17**, 100605 (2005).
[4]W. T. Berggren, M. S. Westphall, and L. M. Smith, "Single-pulse nano-electrospray ionization," Anal. Chem. **74**, 3443 (2002).
[5]C.-Y. Lung, M. D. Barnes, N. Lermer, W. B. Whitten, and J. M. Ramsey, "Single-molecule analysis of ultradilute solutions with guided streams of 1-μm water droplets," Appl. Opt. **38**, 1481 (1999).
[6]A. U. Chen and O. A. Basaran, "A new method for significantly reducing drop radius without reducing nozzle radius in drop-on-demand drop production," Phys. Fluids **14**, L1 (2002).
[7]S. A. Elrod, B. Hadimioglu, B. T. Khuri-Yakub, E. G. Rawson, E. Richley, C. F. Quate, N. N. Mansour, and T. S. Lundgren, "Nozzleless droplet formation with focused acoustic beams," J. Appl. Phys. **65**, 3441 (1989).
[8]D.-Y. Shin, P. Grassia, and B. Derby, "Oscillatory limited compressible fluid flow induced by the radial motion of a thick-walled piezoelectric tube," J. Acoust. Soc. Am. **114**, 1314–1321 (2003).
[9]J. F. Dijksman, "Hydro-acoustics of piezoelectrically driven ink-jet print heads," Flow, Turbul. Combust. **61**, 211–237 (1999).
[10]J. F. Dijksman, "Hydrodynamics of small tubular pumps," J. Fluid Mech. **139**, 173–191 (1984).
[11]J. D. Brock, I. M. Cohen, I. P. Ivanov, H. P. Le, and J. Roy, "Oscillations of an air bubble in an ink jet," J. Imaging Sci. Technol. **10**, 127–129 (1984).
[12]N. P. Hine, "Deaeration system for a high-performance drop-on-demand ink jet," J. Imaging Technol. **17**, 223–227 (1991).
[13]C. E. Brennen, *Cavitation and Bubble Dynamics* (Oxford University Press, Oxford, 1995).
[14]M. M. Fyrillas and A. J. Szeri, "Dissolution or growth of soluble spherical oscillating bubbles," J. Fluid Mech. **277**, 381–407 (1994).
[15]S. Hilgenfeldt, D. Lohse, and M. P. Brenner, "Phase diagrams for sonoluminiscescing bubbles," Phys. Fluids **8**, 2808–2826 (1996).
[16]Flow-3D is CDF software developed by Flow Science Inc., Santa Fe, New Mexico.
[17]C. W. Hirt and B. D. Nichols, "Volume of Fluid (VOF) method for the dynamics of Free Boundaries," J. Comput. Phys. **39**, 201–225 (1981).
[18]J. Eggers, "Nonlinear dynamics and breakup of free-surface flow," Rev. Mod. Phys. **69**, 865–929 (1997).
[19]H. Wijshoff, "Free surface flow and acousto-elastic interaction in piezo inkjet," *Proceedings of NSTI Nanotech 2004 Conference*, 2004, Vol. **2**, pp. 215–218 (http://www.flow3d.com/pdfs/bib2-04.pdf).
[20]X. M. Chen and A. Prosperetti, "Thermal processes in the oscillations of gas bubbles in tubes," J. Acoust. Soc. Am. **104**, 1389–1398 (1998).
[21]H. N. Oguz and A. Prosperetti, "The natural frequency of oscillation of gas bubbles in tubes," J. Acoust. Soc. Am. **103**, 3301–3308 (1998).
[22]X. Geng, H. Yuan, H. N. Oguz, and A. Prosperetti, "The oscillation of gas bubbles in tubes: Experimental results," J. Acoust. Soc. Am. **106**, 674–681 (1999).
[23]J. de Jong *et al.*, in preparation (2006).
[24]In principle, the units of $a(t)$ would be Nm^2/s; however, the signal is linearly converted into a voltage, which is measured in Volts. We decided to omit the units of $a(t)$ in this paper.